

Single Spin Asymmetry Measurements in Semi-Inclusive Pion Electroproduction on a Transversely Polarized Proton Target

X. Jiang (contact person)^a,
Rutgers University, Piscataway, New Jersey.

M. K. Jones
Thomas Jefferson National Accelerator Facility, Newport News, Virginia.

P. Bosted
University of Massachusetts at Amherst, Amherst, Massachusetts.

D. Crabb, D. Day, O. Rondon
University of Virginia, Charlottesville, Virginia.

Abstract: We propose to measure the target single spin asymmetry in the semi-inclusive deep-inelastic $\vec{p}(e, e'\pi^+)$ and $\vec{p}(e, e'\pi^-)$ reaction with a vertically polarized NH_3 target. The goal of this experiment is to provide data on the proton transversity, complementary to the ongoing COMPASS and HERMES measurements and the Hall A neutron transversity experiment E03-004. This experiment focuses on the valence quark region, $x = 0.15 \sim 0.46$, at $Q^2 = 1.45 \sim 3.38 \text{ GeV}^2$. This kinematics is comparable to the HERMES measurement. A large array of calorimeter blocks will be used as the electron detector, to provide out-of-plane angle coverage. A large range of Collins angle ($\phi_h + \phi_S$) is covered while the Sivers angle ($\phi_h - \phi_S$) is optimized close to 90° . The variation of single spin asymmetry over a large range of Collins angle will provide a clear differentiation between the two competing mechanisms—the chiral-even Sivers effect and the chiral-odd Collins effect. Data from this experiment can be used to extract the transversity distributions of u -quark. When combined with data from the expected Hall A neutron transversity experiment, a flavor decomposition of u -quark and d -quark transversity distributions can be performed. The design and development of a vertically polarized target, with a 5.1T super-conducting magnet, to provide 80% target polarization, is the main challenge of a full proposal. A total of 45 days of beam time at 6 GeV in Hall C will be requested when the full proposal is submitted to PAC26.

^aemail: jiang@jlab.org

Contents

1	Introduction	3
2	Physics Motivation	3
2.1	Transversity distributions of the nucleon	3
2.2	Single-spin azimuthal asymmetry in semi-inclusive pion electroproduction	6
2.3	Data from HERMES longitudinal targets and interpretations	9
2.4	Earlier models predicts large transverse proton target single spin asymmetry	13
2.5	Sensitivity of different single spin asymmetry to quark transversity . .	14
3	The Proposed Measurement	15
3.1	Overview	15
3.2	The choice of kinematics	16
3.3	The phase space and Collins angle coverage	17
3.4	The detectors and the trigger	17
3.5	The vertically polarized NH_3 target with a super-conducting magnet.	17
4	Rate Estimate and Expected Beam Time	19
4.1	Cross section and rate estimate	19
4.2	Beam time and coincidence rate	20
5	Expected Results	21
5.1	Single-spin asymmetry	21
5.2	By-products	22
6	Summary	22

1 Introduction

The topic of single spin asymmetry in semi-inclusive deep-inelastic scattering has received much attention in the past two years¹. This attention was stimulated by the data from HERMES run-I, in which non-vanishing azimuthal asymmetries were reported in pion production on a polarized proton target^{2,3}. For the first time, it appears that an observable can be attributed to the effect of the quark transverse spin, and a time-reversal odd quark fragmentation process can be identified. It was highly expected that when HERMES finishes data taking on its transversely polarized proton target, information on the u -quark transversity distribution and its T -odd fragmentation function will become available⁴.

Recently HERMES preliminary data of the transverse target becomes available, with limited statistics (600k SIDIS events total), it was very surprising and completely out of expectations. The π^+ Collins SSA turned out to be rather small, positive at a few percent level, compared to the earlier expectations of 15 \sim 30%. The π^- Collins SSA shows a negative trend, compared with the earlier expectations of small asymmetry, as shown in Fig. 1. The Sivers SSA also turned out to be rather small as shown in Fig. 2. Furthermore, it becomes a concern that the exclusive ρ production could have contaminated the HERMES semi-inclusive data. HERMES Monte Carlo simulation indicated that events from ρ production channel can not be reliably eliminated by the regular HERMES kinematics cuts, without losing the majority of the event sample.

It is crucial to independently verify the HERMES results with high statistics data and perhaps at a different kinematics condition, where the exclusive ρ contribution can be less significant. This intended experiment is designed to provide high statistic data on proton single spin asymmetry through $\vec{p}(e, e'\pi^+)X$ and $\vec{p}(e, e'\pi^-)X$ measurement on a vertically polarized NH_3 target. At $x = 0.15 \sim 0.46$, at $Q^2 = 1.45 \sim 3.38$ GeV^2 comparable to the HERMES kinematics. Data from this experiment can be used to extract the transversity distributions of u -quark. When combined with data from the expected Hall A neutron transversity experiment, a flavor decomposition of u -quark and d -quark transversity distributions can be performed.

2 Physics Motivation

2.1 Transversity distributions of the nucleon

At the leading twist, three fundamental quark distributions provide a complete description of quark momentum and spin in the nucleon⁵. The unpolarized quark distributions are well-known, thanks to the extensive deep-inelastic scattering (DIS) data collected over the last three decades. The longitudinal polarized quark distributions are also reasonably known from the polarized DIS data, and more recently from the semi-inclusive deep-inelastic scattering (SIDIS) data of HERMES and SMC. The third type of distribution, the “transversity distribution”, despite strong theoretical

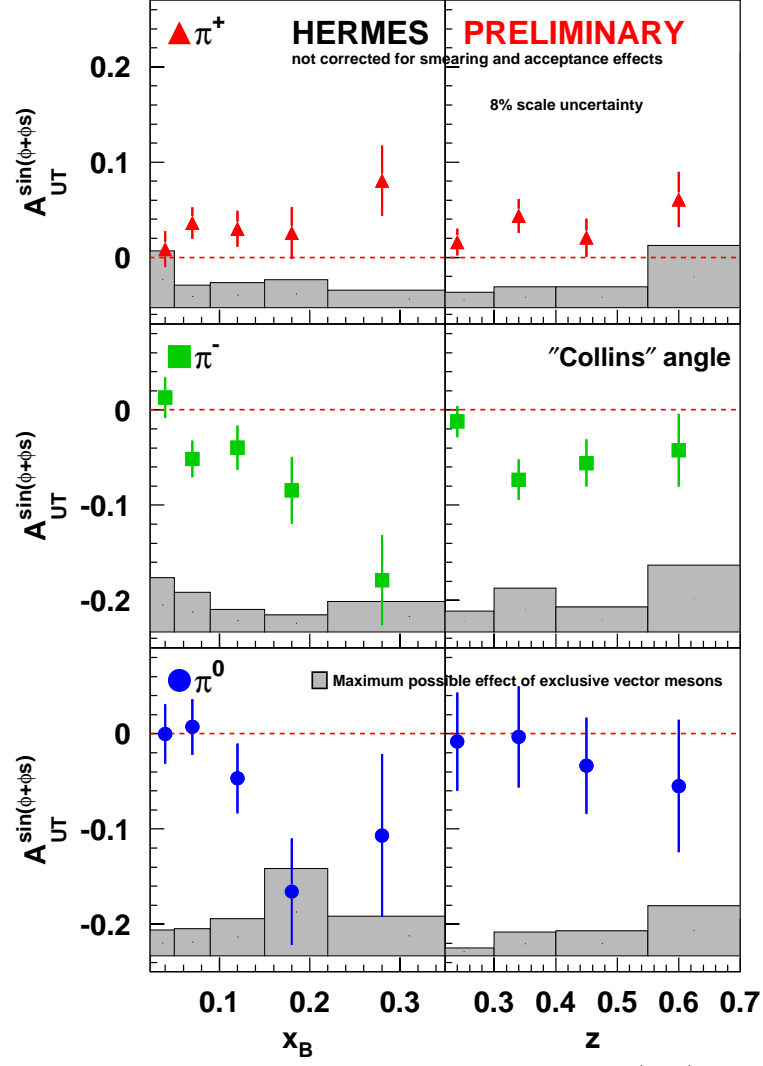


Figure 1: HERMES transverse target SSA of Collins type ($\sin(\phi_h + \phi_s)$).

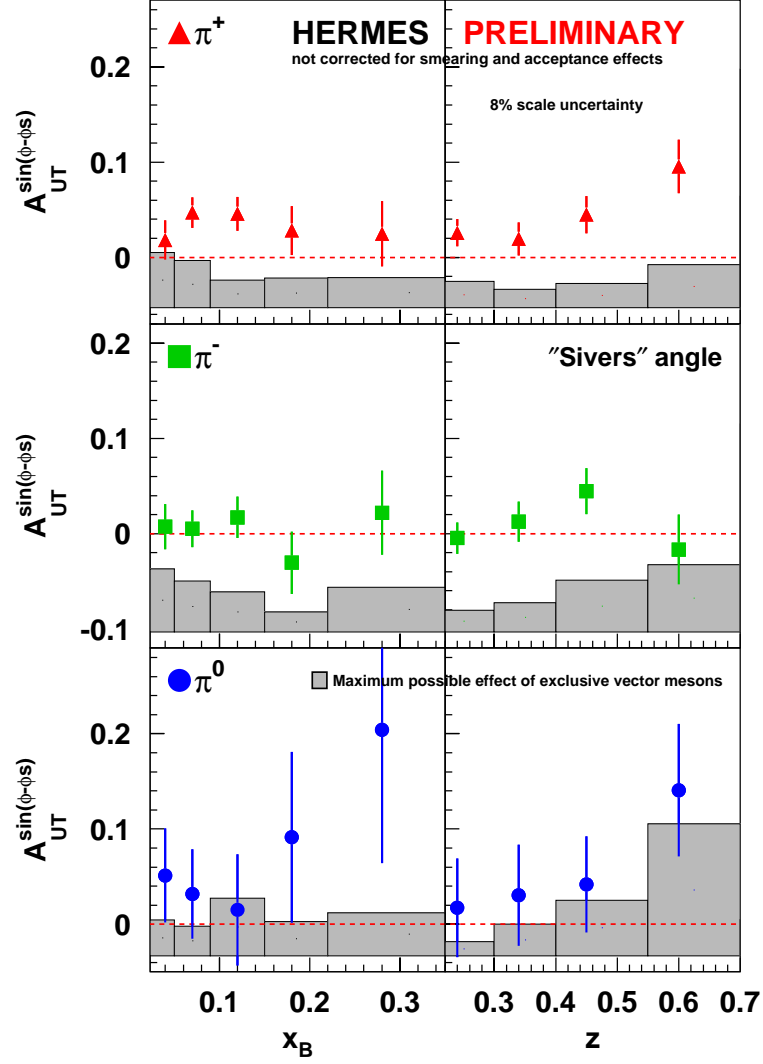


Figure 2: HERMES transverse target SSA of Sivers type ($\sin(\phi_h - \phi_s)$).

and experimental interest, remains practically unknown.

The transversity distribution (h_1^q) can be interpreted as the probability to find a transversely polarized quark in a transversely polarized nucleon⁶. Unlike the unpolarized and longitudinally polarized distributions (f_1^q and g_1^q), which are chiral-even quantities, the transversity distribution has a chiral-odd structure. Due to this chiral-odd nature, the transversity distribution can not be accessed through inclusive DIS processes because an additional chiral-odd object is required.

The transversity distributions have many interesting theoretical aspects, related to general properties of QCD as well as to the structure of the nucleon:

- In the non-relativistic quark model (no spin-orbit interaction), where boosts and rotations commute, the transversity distributions are identical to the longitudinally polarized distributions. Since the quarks inside the nucleon cannot be non-relativistic, the transversity distributions provide a detailed measure of the relativistic nature of the quarks inside the nucleon.
- The transversity distribution is expected to follow a valence like behavior. Since the transversity of gluons in a nucleon does not exist, the transversity distribution does not mix with gluons in its evolution, and is expected to follow a simple evolution as a flavor non-singlet quantity⁷.
- The transversity obeys some important inequalities. The first, $|h_1^q| \leq f_1^q$, follows from its interpretation as a difference of probabilities. The second (Soffer's bound) has its origins in the positivity of helicity amplitudes⁸: $|h_1^q| \leq \frac{1}{2}(f_1^q + g_1^q)$.
- The lowest moment of h_1^q measures a simple local operator analogous to the axial charge, known as the “tensor charge”. Unlike its vector and axial equivalents, the tensor charge evolves with Q^2 .

2.2 Single-spin azimuthal asymmetry in semi-inclusive pion electroproduction

It has been proposed that the transversity distribution can manifest itself in SIDIS reactions through the Collins effect⁹, where the transversity distribution can be probed through a chiral-odd T -odd quark fragmentation function—the Collins function. Indeed, an analysis of $Z^0 \rightarrow 2$ jets decay indicated that the Collins fragmentation function has a sizable magnitude¹⁰. Recent results on target single spin azimuthal asymmetries in SIDIS reactions from HERMES and SMC¹¹ offered the first glimpse of possible effects caused by the transversity distribution.

The kinematics and the coordinate definition are illustrated in Fig. 3. We define E' as the energy of the scattered electron and θ_e is the scattering angle, $\nu = E - E'$ is the energy transfer. The Bjorken- x , which indicates the fractional momentum carried by the struck quark, is defined as: $x = Q^2/(2\nu M_N)$, M_N is the nucleon mass. The momentum of the outgoing pion is p_π and the fraction of the virtual photon energy carried by the pion is: $z = E_\pi/\nu$. W is the invariant mass of the

whole hadronic system and W' is the invariant mass of the hadronic system without the detected pion. We have:

$$\begin{aligned} W^2 &= M_N^2 + Q^2 \left(\frac{1}{x} - 1 \right), \\ W'^2 &= (M_N + \nu - E_\pi)^2 - |\vec{q} - \vec{p}_\pi|^2. \end{aligned} \quad (1)$$

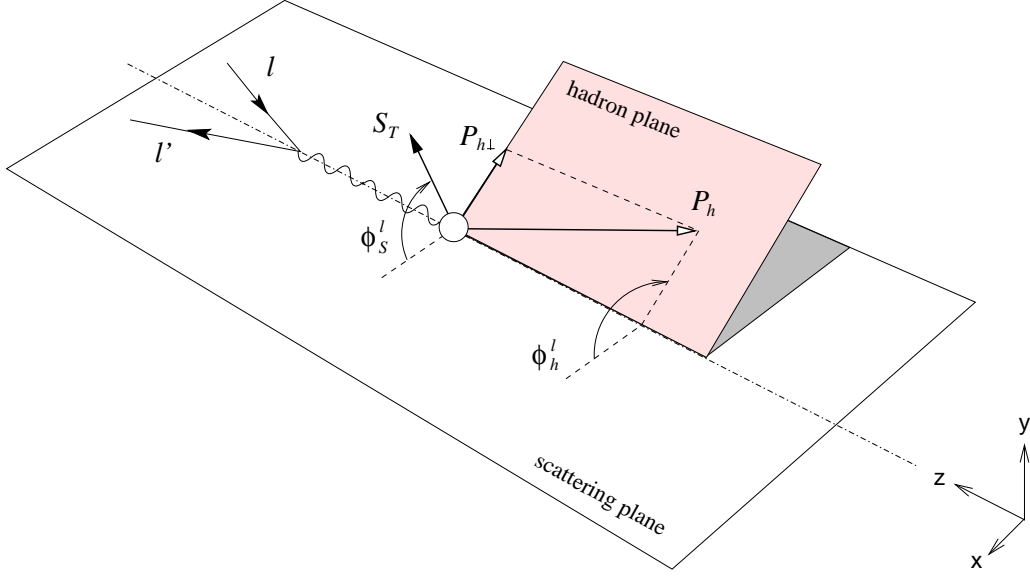


Figure 3: The definition of the coordinates.

The pion transverse momentum relative to \vec{q} is labeled as $P_{h\perp}$. At the leading order, when h is a spin zero particle, the spin-dependent cross section^{12,13,14} is:

$$\begin{aligned} d^6\sigma^{LO} &= \frac{d\sigma^{\ell+N \rightarrow \ell'+h+X}}{dx dy d\phi^\ell dz d^2\mathbf{P}_{h\perp}} = \frac{4\pi\alpha^2 s x}{Q^4} \times \\ &\left\{ \left[1 + (1-y)^2 \right] \sum_{q,\bar{q}} e_q^2 f_1^q(x) D_1^q(z, \mathbf{P}_{h\perp}^2) \right. \\ &+ (1-y) \frac{P_{h\perp}^2}{4z^2 M_N M_h} \cos(2\phi_h^\ell) \sum_{q,\bar{q}} e_q^2 h_1^{\perp(1)q}(x) H_1^{\perp q}(z, \mathbf{P}_{h\perp}^2) \\ &- |\mathbf{S}_L| (1-y) \frac{P_{h\perp}^2}{4z^2 M_N M_h} \sin(2\phi_h^\ell) \sum_{q,\bar{q}} e_q^2 h_{1L}^{\perp(1)q}(x) H_1^{\perp q}(z, \mathbf{P}_{h\perp}^2) \\ &+ |\mathbf{S}_T| (1-y) \frac{P_{h\perp}}{z M_h} \sin(\phi_h^\ell + \phi_S^\ell) \sum_{q,\bar{q}} e_q^2 h_1^q(x) H_1^{\perp q}(z, \mathbf{P}_{h\perp}^2) \\ &\left. + |\mathbf{S}_T| \left(1 - y + \frac{1}{2} y^2 \right) \frac{P_{h\perp}}{z M_N} \sin(\phi_h^\ell - \phi_S^\ell) \sum_{q,\bar{q}} e_q^2 f_{1T}^{\perp(1)q}(x) D_1^q(z, \mathbf{P}_{h\perp}^2) \right\} \end{aligned}$$

$$\begin{aligned}
& + |\mathbf{S}_T| (1-y) \frac{P_{h\perp}^3}{6z^3 M_N^2 M_h} \sin(3\phi_h^\ell - \phi_S^\ell) \sum_{q,\bar{q}} e_q^2 h_{1T}^{\perp(2)q}(x) H_1^{\perp q}(z, \mathbf{P}_{h\perp}^2) \\
& + \lambda_e |\mathbf{S}_L| y (1 - \frac{1}{2}y) \sum_{q,\bar{q}} e_q^2 g_1^q(x) D_1^q(z, \mathbf{P}_{h\perp}^2) \\
& + \lambda_e |\mathbf{S}_T| y (1 - \frac{1}{2}y) \frac{P_{h\perp}}{zM_N} \cos(\phi_h^\ell - \phi_S^\ell) \sum_{q,\bar{q}} e_q^2 g_{1T}^{(1)q}(x) D_1^q(z, \mathbf{P}_{h\perp}^2) \Big\}. \quad (2)
\end{aligned}$$

where $|\mathbf{S}_L|$ and $|\mathbf{S}_T|$ are the longitudinal and transverse spin component, λ_e is the electron helicity. Azimuthal angles are defined relative to the lepton plane, e.g. $\phi_h^\ell = \phi_h - \phi^\ell$ is the angle between the hadron plane ($\vec{P}_h \wedge \vec{q}$) and the lepton plane. $\phi_S^\ell = \phi_S - \phi^\ell$ is the angle between the $\vec{S} \wedge \vec{q}$ plane and the lepton plane.

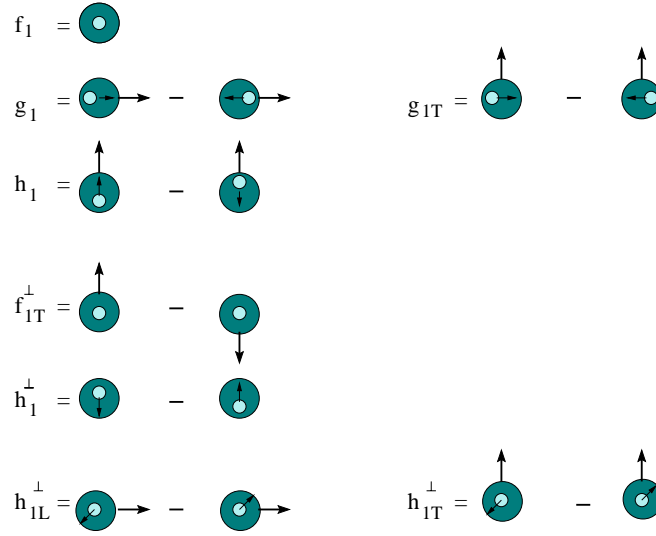


Figure 4: A pictorial representation of the distribution functions[?]. Three functions, $f_1^q(x)$, $g_1^q(x)$ and $h_1^q(x)$ survive the integration of quark \mathbf{p}_T .

Fig. 4 gives a pictorial representation of the distribution functions. The distribution $f_1^q(x)$ is the probability of finding an unpolarized quark in an unpolarized nucleon; $g_1^q(x)$ is for a longitudinally polarized quark in a longitudinally polarized nucleon and $h_1^q(x)$ is for a transversely polarized quark in a transversely polarized nucleon. These three functions survive the integration of intrinsic quark transverse momentum \mathbf{p}_T in the initial nucleon. The corresponding \mathbf{p}_T dependent distributions are $f_{1T}^{\perp q}$, $g_{1T}^{\perp q}$, $h_{1L}^{\perp q}$, $h_{1T}^{\perp q}$ and $h_{1L}^{\perp q}$. They only survive the \mathbf{p}_T integration after weighting with $(\mathbf{p}_T^2/2M_N^2)^n$. Such weighting is indicated by a superscript (n) in Eq. 2.

With unpolarized beam and a transversely polarized target, three terms in Eq. 2 contribute to the single target-spin asymmetry. The $\sin(\phi_h^\ell + \phi_S^\ell)$ term is the Collins effect, which involves the chiral-odd transversity distribution $h_1^a(x)$ and the chiral-odd and T -odd Collins fragmentation function $H_{1T}^{\perp a}$. The $\sin(\phi_h^\ell - \phi_S^\ell)$ term is the Sivers effect, which involves the chiral-even T -odd Sivers distribution function $f_{1T}^{\perp a}(x)$

and the regular fragmentation function D_1^a . The Siverson function is non-vanishing at the leading twist^{17,18}, and is due to the asymmetric distribution of quark transverse momentum in a nucleon. The $\sin(3\phi_h^\ell - \phi_S^\ell)$ term, compared to the Collins term, contains an extra factor of $\frac{1}{6}(P_{h\perp}/zM_N)^2$ which amounts to only 0.03–0.13 in this experiment. In addition, one expects that $h_{1T}^{\perp(2)a}(x) \ll h_1^a(x)$ due to quark transverse momentum weighting. Therefore, we assume contribution from the $\sin(3\phi_h^\ell - \phi_S^\ell)$ term is negligible. Similarly, the $\cos(2\phi_h^\ell)$ term of the unpolarized cross section can be neglected in the asymmetry expression. For a 100% polarized nucleon, the transverse momentum dependent single target-spin asymmetry is:

$$\begin{aligned}
A_T(x, z, \mathbf{P}_{h\perp}^2) &= (A_T)_{Collins} + (A_T)_{Sivers} \\
&= \frac{1-y}{1-y+\frac{1}{2}y^2} \cdot \frac{P_{h\perp}}{zM_h} \sin(\phi_h^\ell + \phi_S^\ell) \cdot \frac{\sum_{q,\bar{q}} e_q^2 h_1^q(x) H_1^{\perp q}(z, \mathbf{P}_{h\perp}^2)}{\sum_{q,\bar{q}} e_q^2 f_1^q(x) D_1^q(z, \mathbf{P}_{h\perp}^2)} \\
&\quad + \frac{P_{h\perp}}{zM_N} \sin(\phi_h^\ell - \phi_S^\ell) \cdot \frac{\sum_{q,\bar{q}} e_q^2 f_{1T}^{\perp(1)q}(x) D_1^q(z, \mathbf{P}_{h\perp}^2)}{\sum_{q,\bar{q}} e_q^2 f_1^q(x) D_1^q(z, \mathbf{P}_{h\perp}^2)} \quad (3)
\end{aligned}$$

2.3 Data from HERMES longitudinal targets and interpretations

The HERMES collaboration has reported^{2,3} the single spin azimuthal asymmetries for charged and neutral pion electroproduction based on a SIDIS data sample of $\langle Q^2 \rangle = 2.5 \text{ GeV}^2$ on proton and deuteron. Using an unpolarized positron beam on a longitudinally polarized target (such that $\phi_S^l = 0$), the cross section was found to have a $\sin\phi_h^l$ dependence in both π^+ and π^0 production as shown in Fig. 5. The deuteron longitudinal target SSA data is shown in Fig. 6. This single spin asymmetry can be expressed as the analyzing power in the $\sin\phi_h^l$ moment, and the result is shown in Fig. 7 as a function of pion fractional energy z , Bjorken x , and the pion transverse momentum P_\perp . The $\sin\phi_h^l$ moment for an unpolarized (U) positron scattered off a longitudinally (L) polarized target contains two main contributions

$$\begin{aligned}
\langle \sin\phi_h^l \rangle &\propto 4S_L \frac{M}{Q} (2-y) \sqrt{1-y} \sum_{q,\bar{q}} e_q^2 \left(h_L^q(x) H_1^{\perp q}(z) - h_{1L}^{\perp q(1)}(x) \tilde{H}(z) \right) \\
&\quad - 2S_T (1-y) \sum_{q,\bar{q}} e_q^2 h_1^q(x) H_1^{\perp q}(z). \quad (4)
\end{aligned}$$

For the HERMES experiment with a longitudinally polarized target, the transverse component is nonzero with a mean value of $S_T \approx 0.15$. The observed azimuthal asymmetry could be a combined effect of h_1^q —the twist-2 transversity distribution, and h_L^q —the twist-3 distribution function in the longitudinally polarized nucleon¹⁵. Figure 7 shows that a model calculation^{15,16} reproduces the z , x , and p_\perp dependences of the π^0 asymmetry. The striking difference between the π^+ and π^- analyzing power suggests that the u -quark dominates the proton asymmetry.

If the azimuthal asymmetry observed by HERMES is indeed caused by the h_1^q transversity distribution, a much larger asymmetry is expected for a transversely

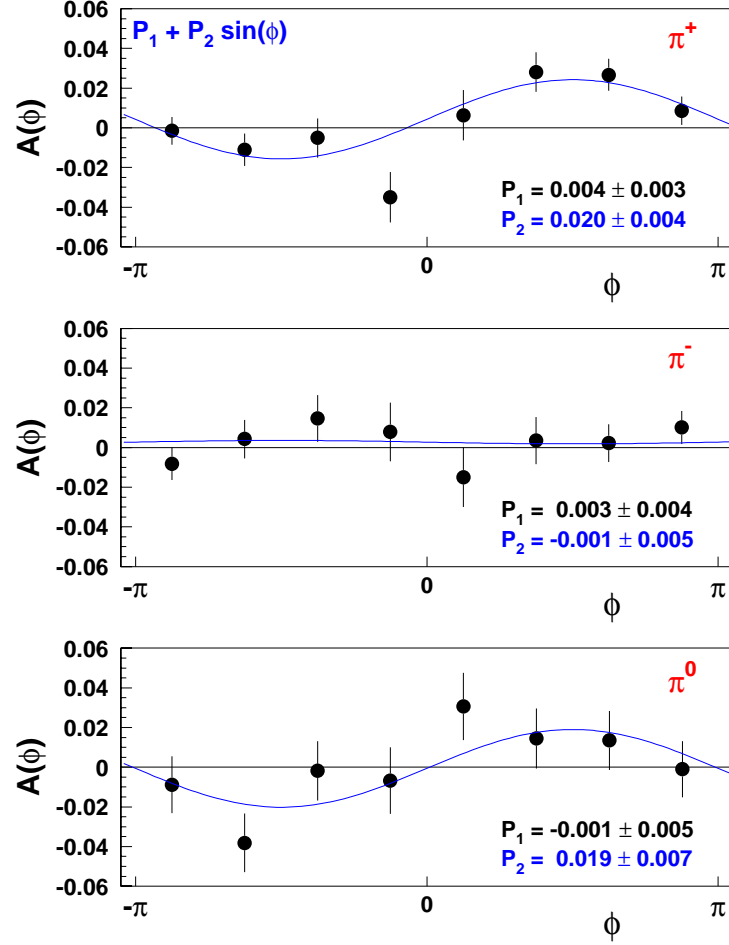


Figure 5: Analyzing power as a function of $\phi = \phi_h^l$ from HERMES^{2,3} proton target measurements. Solid lines indicate fits of $P_1 + P_2 \sin(\phi_h^l)$.

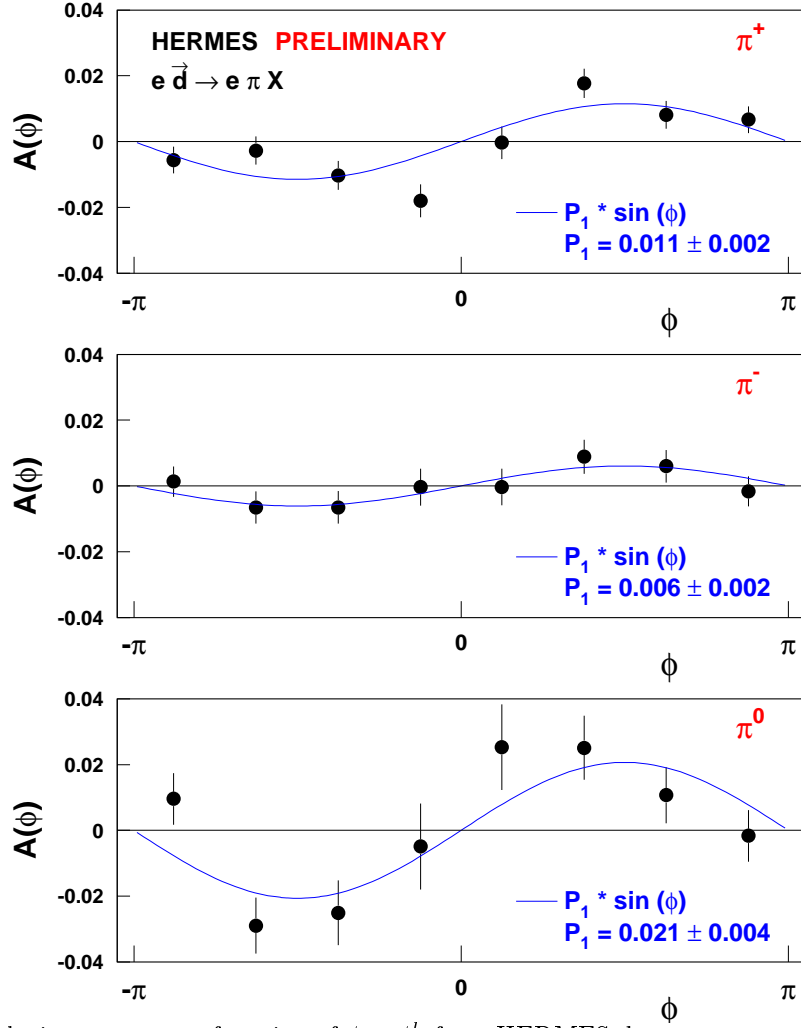


Figure 6: Analyzing power as a function of $\phi = \phi_h^l$ from HERMES deuteron target measurements. Solid lines indicate fits of $P_1 + P_2 \sin(\phi_h^l)$.

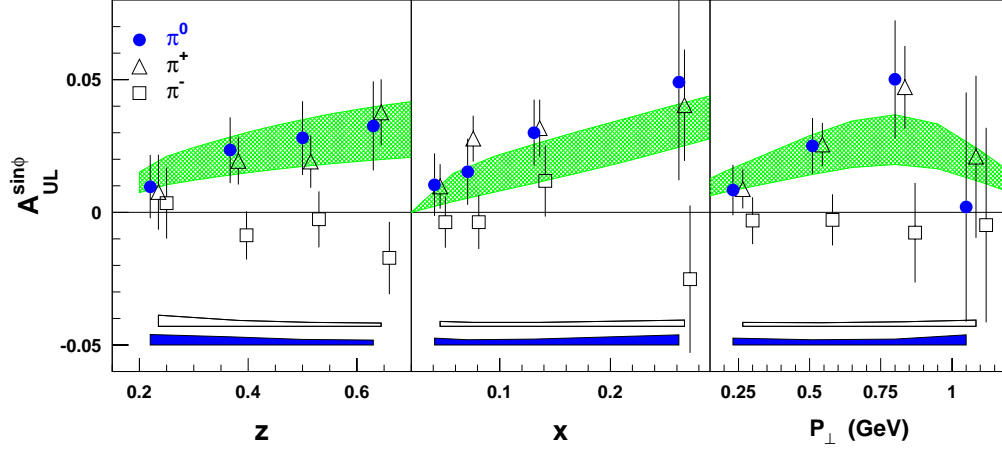


Figure 7: Analyzing power in the $\sin\phi_h^l$ moment from HERMES^{2,3} proton target measurements. Solid bands that fit the data assume that the transversity distributions range from $h_1 = g_1$ to $h_1 = (f_1 + g_1)/2$. Error bars include the statistical uncertainty only. The bands at the bottom of the panels represent the systematic uncertainties.

polarized target. An earlier SMC measurement on a transversely polarized proton target, as shown in Fig. 8, had limited statistics and was inconclusive¹¹. The HERMES run-II plans to have a dedicated two-year transversely polarized proton target run to measure the shape of $h_1^u(x)$ (and $H_1^u(z)$).

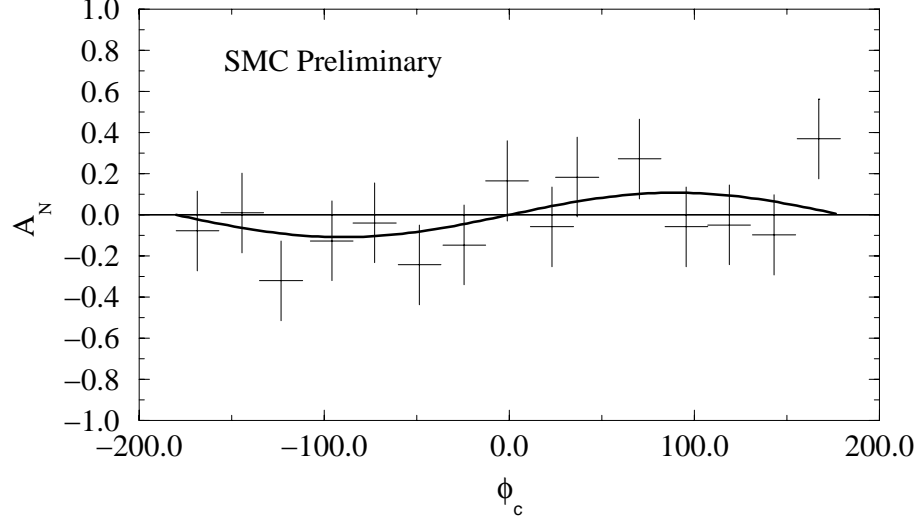


Figure 8: Analyzing power as a function of $\phi_c = \phi_h^l + \phi_S^l$ from SMC¹¹ on a transversely polarized proton target.

Complicating the situation, it was found that a chiral-even mechanism previously considered forbidden (the Sivers effect), is actually allowed in SIDIS, adding contributions in competition with the Collins effect. Using a QCD motivated quark-diquark model, Brodsky *et al.*¹⁷ demonstrated that the final state interactions from gluon exchange between the outgoing quark and the target spectator leads to a

sizable single spin asymmetry. This quark final state interaction is interpreted¹⁸ as giving rise to the chiral-even T -odd Sivers function¹⁹. It was further demonstrated²⁰ that the quark final-state interactions can be fully accounted for in the light-cone approach. Both the Collins effect and the Sivers effect can contribute to the observed single spin asymmetry.

Fortunately, in a measurement involving a transversely polarized target, the two competing mechanisms can be distinguished by observing single spin asymmetry as a function of the Collins angle. The Collins effect, which involves transversity distributions and chiral-odd fragmentation functions, contributes a $\sin(\phi_h^l + \phi_S^l)$ dependence to the cross section. The Sivers effect, which involves chiral-even T -odd distribution functions and chiral-even fragmentation functions, contributes a $\sin(\phi_h^l - \phi_S^l)$ dependence. In addition, the two competing contributions have different kinematic dependences. The Collins effect depends on a kinematic factor of $(1-y)/(1-y+\frac{1}{2}y^2)$ and is strongly correlated with z , but the Sivers effect is independent of y and not strongly correlated with z , where $y = \nu/E$ and $z = E_\pi/\nu$. Therefore, with a transversely polarized target and a broad coverage in Collins angles, y and z , such as in HERMES run-II and in this experiment, differentiation between the Collins effect and the Sivers effect becomes possible.

2.4 Earlier models predicts large transverse proton target single spin asymmetry

From Eq. 3, assuming only the Collins effect contributes, the azimuthal asymmetry A_T is²¹:

$$A_T(x, z, \mathbf{P}_{h\perp}^2) = \frac{1-y}{1-y+\frac{1}{2}y^2} \cdot \left(\frac{|\mathbf{P}_\perp|}{zM_h} \right) \cdot \frac{\sum_q h_1^q(x) H_1^{\perp q}(z, \mathbf{P}_\perp^2)}{\sum_q f_1^q(x) D_1^q(z, \mathbf{P}_\perp^2)}, \quad (5)$$

Omitting the explicit Q^2 notation, the transverse momentum dependent fragmentation function $D_1^q(z, \mathbf{P}_\perp^2)$ relates to the normal fragmentation function through the integration of the scattered quark transverse momentum $\mathbf{k}_T = \mathbf{P}_\perp/z$:

$$z^2 \int d^2\mathbf{k}_T D_1^q(z, \mathbf{P}_\perp^2) \equiv D_1^q(z). \quad (6)$$

Collins suggested¹⁸ that the analyzing power in transversely polarized quark fragmentation follow:

$$A_C(z, k_T) \equiv \frac{|\mathbf{k}_T| H_1^{\perp q}(z, \mathbf{P}_\perp^2)}{M_h D_1^q(z, \mathbf{P}_\perp^2)} = \frac{M_C |\mathbf{k}_T|}{M_C^2 + |\mathbf{k}_T|^2}, \quad (7)$$

with $M_C = 0.3 \sim 1.0$ GeV. HERMES analysis takes $M_C = 0.7$ GeV as a rough guess⁴, which we will follow in our numerical estimates. The transverse momentum dependence of $D_1^q(z, \mathbf{P}_\perp^2)$ is assumed to have a Gaussian type shape:

$$D_1^q(z, \mathbf{P}_\perp^2) = D_1^q(z) \cdot \frac{R^2}{\pi z^2} \exp(-R^2 \mathbf{P}_\perp^2 / z^2), \quad (8)$$

with $R^2 = z^2/b^2$, and b^2 is the mean-square momentum the hadron acquires in the quark fragmentation process with $b^2 = 0.25 \text{ (GeV/c)}^2$ according to HERMES²².

The predictions²¹ of A_T from a quark diquark model and a PQCD based analysis are shown in Fig. 9 for π^+ and π^- on a proton. The calculation in Fig. 9 has been integrated over z and the pion transverse momentum P_\perp to demonstrate the x -dependence at the HERMES kinematics of $Q^2 = 2.5 \text{ GeV}^2$. A sizable asymmetry on the proton is expected in the valence quark region. In this experiment we will focus on the valence quark region ($x = 0.15 \sim 0.46$) and measure $\vec{p}(e, e'\pi^+)X$ and $\vec{p}(e, e'\pi^-)X$ reactions with a vertically polarized NH_3 target.

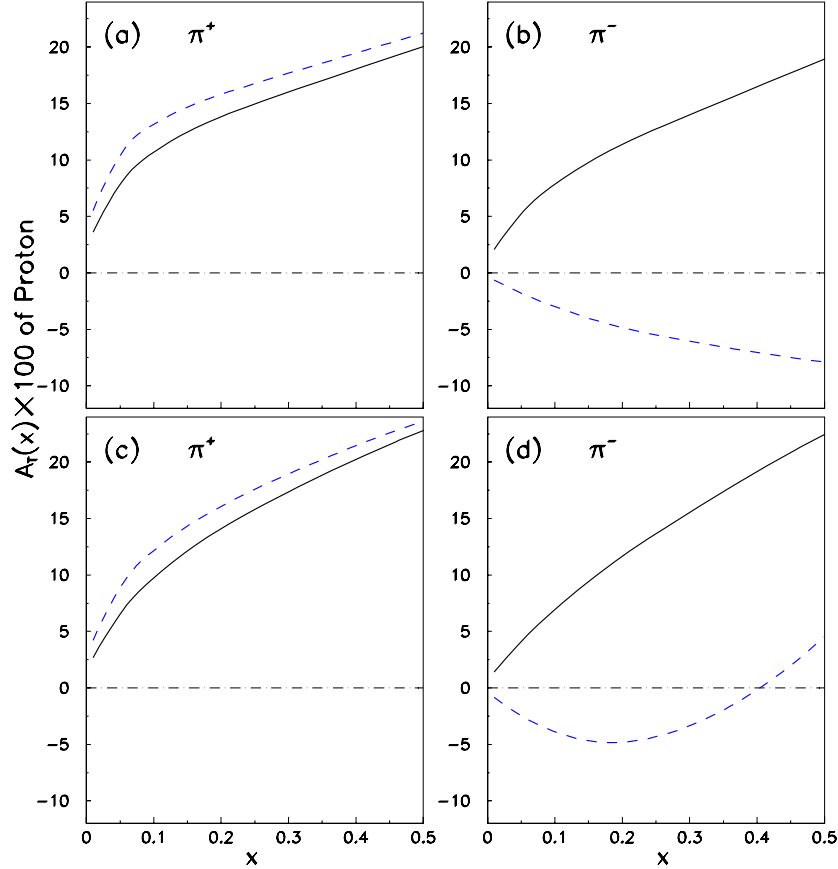


Figure 9: Transverse single-spin asymmetry for the proton target²¹. The upper row corresponds to predictions of quark diquark model, and the lower row corresponding predictions of the PQCD based analysis. The solid curves are the calculated results with both favored and unfavored fragmentation, the dashed curves are the results with only favored fragmentation.

2.5 Sensitivity of different single spin asymmetry to quark transversity

The sensitivity of different single spin asymmetry to quark transversity distributions is illustrated in Fig. 10. The solid red curves correspond to the Soffer boundary,

the dashed black curves are for the favored fragmentation only (one kind of quark contributes), and the solid curves include contributions from both u -quark and d -quark. The factor D_{nn} is the kinematics factor. The curves are calculated for $Q^2 = 2.0 \text{ GeV}^2$, $z=0.5$ and $P_t = 0.35 \text{ GeV}/c$, as in this experiment. The AAC polarized distributions are used while assuming $\delta q = \Delta q$.

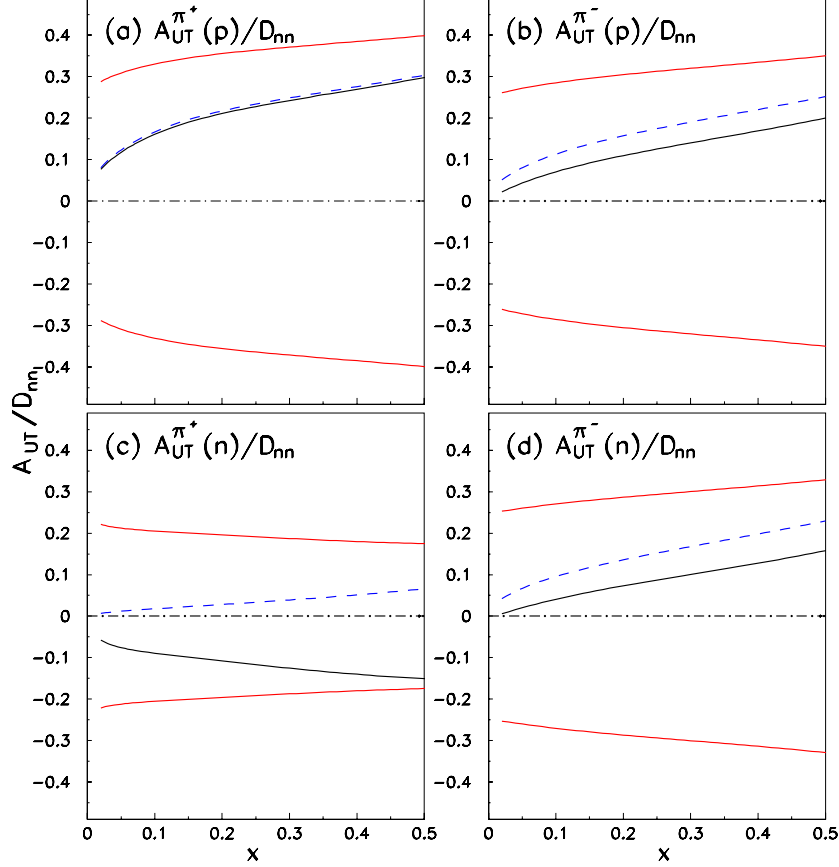


Figure 10: Sensitivity of different single-spin asymmetries to quark transversity distributions. Different curves are explained in the text.

3 The Proposed Measurement

3.1 Overview

We plan to study the target single spin asymmetry (SSA) in the semi-inclusive deep-inelastic $\vec{p}(e, e'\pi^+)X$ and $\vec{p}(e, e'\pi^-)X$ reaction using a new system of vertically polarized NH_3 target in Hall C and a 6 GeV beam. The target thickness will be 3.0 cm and the average beam current will be $\approx 80 \text{ nA}$. A new super-conducting magnet need to be designed and built in order to provide a 5.1T holding field for the polarized target. An average target polarization of 80% is expected as in the other Hall C

polarized target experiment. The experiment will use the Hall C spectrometer HMS

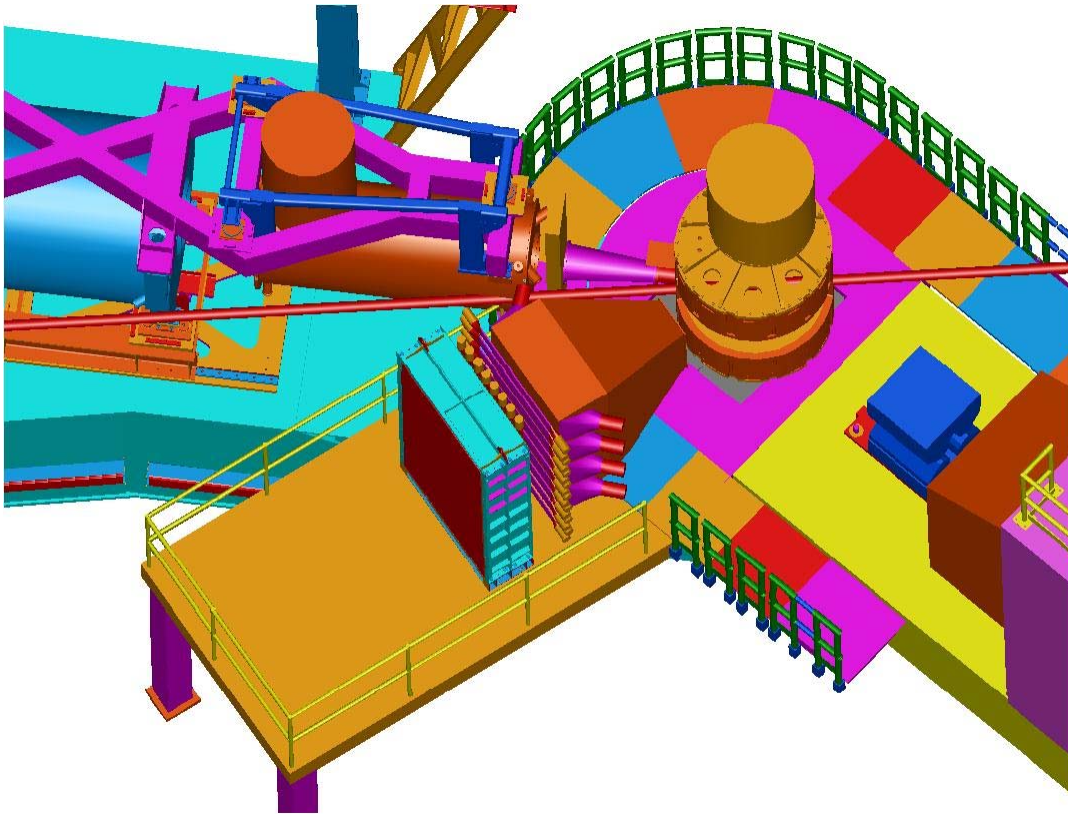


Figure 11: A top view of the Hall C floor arrangement. The thick red line represents the beam which is incident from the right (the beam dump is to the left of the picture). The electron-arm detector, with the extended BigCal on the back and the extended gas Cherenkov in the front, is at 30° beam left. The HMS spectrometer is shown at 16.0° beam right. The SOS spectrometer is parked on beam left, not involved in this experiment.

situated at 16° as the hadron arm on beam right, and use a 50% extended lead-glass calorimeter array BigCal at 30° beam-left as the electron detector. A new system of vertically polarized NH_3 target will be used. The Hall C floor arrangement is illustrated in Fig. 11.

3.2 The choice of kinematics

Similar to the Hall A neutron transversity experiment, here we chose to cover the highest possible W with a 6 GeV beam. We chose to detect the leading fragmentation pion which carries $z \sim 0.50$ of the energy transfer to favor the current fragmentation. The value of W' is also chosen to be as high as possible to avoid contributions from resonance structures. The central kinematic values for each x -bin are listed in Table 1. The values of W' and z for each x -bin are listed in Table 1.

Table 1: Central kinematics for each x -bin for a beam energy of $E = 6.0$ GeV. One BigCal and HMS setting cover all the kinematics listed. E' and θ_e are the central electron momentum and angle, θ_q indicates the direction of \vec{q} . Single arm electron rates for each x -bin are listed. The charged pion angle is 16° .

E' GeV	θ_e deg.	$\langle x \rangle$	W GeV	Q^2 GeV ²	θ_q deg.	Rate of (e, e') on NH ₃ in Hz	p_π GeV/c	z	W' GeV
							$\theta_\pi = 16.0^\circ$		
0.90	30	0.15	3.00	1.45	4.9	488	2.20	0.43	2.24
1.30	30	0.24	2.76	2.09	7.6	327	2.20	0.47	2.04
1.70	30	0.34	2.49	2.73	10.6	208	2.20	0.51	1.82
2.10	30	0.46	2.20	3.38	14.1	111	2.20	0.57	1.57

3.3 The phase space and Collins angle coverage

The phase space coverage is obtained from a detailed Monte Carlo simulation which includes target field, realistic spectrometer models as well as target and detector geometry. The angular coverage of $\phi_h + \phi_S$ and $\phi_h - \phi_S$ is shown in Fig. 12.

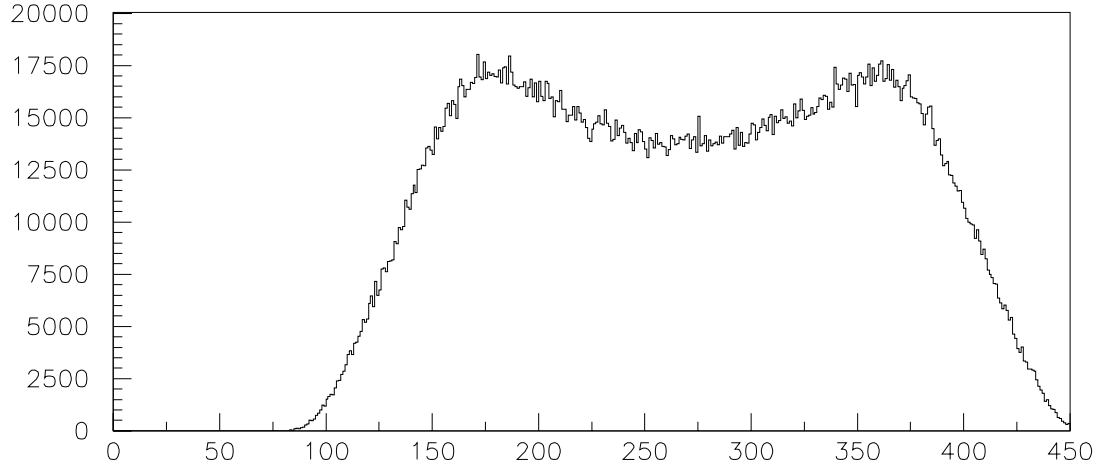
3.4 The detectors and the trigger

The electron detector will be an extended version of the calorimeter array BigCal as in the SANE proposal and the GEP-III proposal. We plan to obtain more lead glass blocks to cover an extra area of 120cm by 108cm. The additional blocks will be added on top of BigCal to increase the vertical angle coverage, such that the Collins angle coverage will span from 130° to 400° . The background rates on the calorimeter has been calculated using the Monte Carlo simulation code GDINR²³, and including the effects of target field and target material. The singles rate will be similar to that of the SANE experiment, once a gap of 24 cm is left in the horizontal direction. The target field will be set in a way that the low energy electrons, which dominate the background, will be bend to beam right (HMS side) to reduce the low energy electron background on the calorimeter.

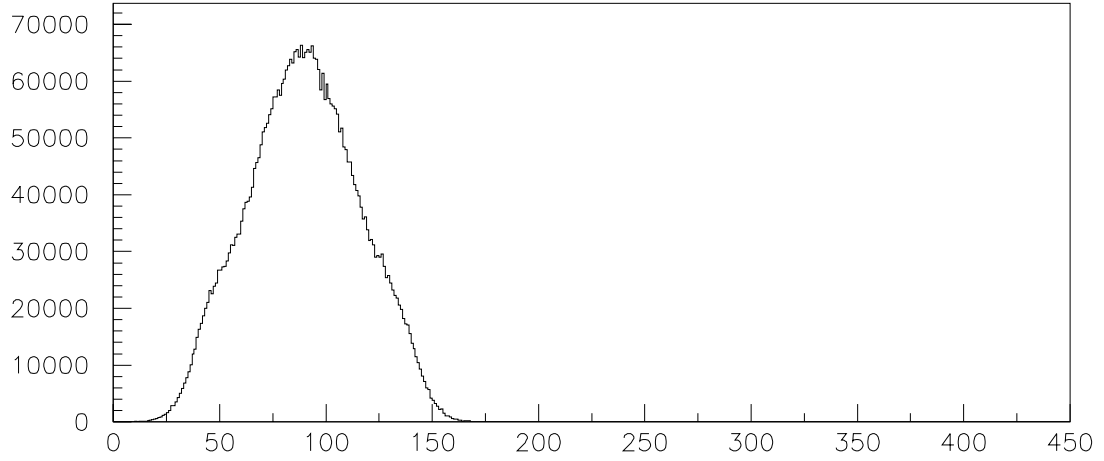
The hadron arm spectrometer HMS will be set at 16° , at a momentum of 2.2 GeV/c. The momentum acceptance of HMS is close to $\pm 10\%$. Both positive and negative HMS settings will be taken in this experiment. The trigger will be provided by HMS alone. For each trigger, the calorimeter hit-blocks ADC and TDC information will be read out for offline analysis.

3.5 The vertically polarized NH₃ target with a super-conducting magnet.

Magnets with large horizontal and vertical acceptance are difficult to design and fabricate. Iron magnets can have very large horizontal acceptances and adequate vertical acceptances for most experiments but can only operate at fields of about 2.5T which with a helium refrigerator operating at about 1K lead to polarizations of



phizlh+phizls1 phase space



phizlh-phizls1 phase space

Figure 12: Available phase space in the Collins angle (top) and the Sivers angle. Event numbers are not to scale.

up to about 45%. Using a dilution refrigerator or ^3He refrigerator, polarizations of up to 90% are possible, but the high beam intensity requirements of the transversity experiments, precludes the use of such refrigerators. A ^4He refrigerator together with a high field magnet provides a path to high polarizations.

The available super-conducting magnets have mostly been optimized for experiments with the longitudinal polarization with some compromises made to provide access with a transverse, in-plane polarization direction. We are investigating the possibility of obtaining a super-conducting magnet with a transverse vertical field and with a vertical opening angle of ± 30 degrees and horizontal opening angle of ± 45 degrees. This is under study. Another plan is to investigate whether a race-track coil design is feasible at the 5T level. Among other possibilities, this would allow longer targets than possible with the conventional coil design. Working closely together with Oxford Instrument, we expected to come up with a technical design report and a cost estimation for a super conducting magnet in about six months. Once the design work has been finished, the manufacturing of the magnet is expected to take $18 \sim 24$ months.

4 Rate Estimate and Expected Beam Time

4.1 Cross section and rate estimate

For the rate estimation, we assumed a NH_3 target thickness of 3 cm, a beam current of 80 nA. The extended BigCal with a solid angle coverage of 300 msr is assumed. The HMS spectrometer, operated under the “large solid angle tune” is assumed to be 10 msr, as suggested by Dr. Y. Chen’s HMS optics calculation.

The model of coincident cross sections has the following inputs:

- The inclusive $p(e, e')$ cross section.
- A parameterization of the fragmentation functions $D^+(z)$ and $D^-(z)$.
- A model of the transverse momentum distributions of pions as fragmentation products.

The inclusive deep inelastic (e, e') cross section can be expressed in the quark parton model as:

$$\frac{d^2\sigma}{d\Omega dE'} = \frac{\alpha^2(1 + (1 - y)^2)}{sxy^2} \frac{E'}{M_N \nu} \sum_{q, \bar{q}} e_q^2 f_1^q(x), \quad (9)$$

where $s = 2E M_N + M_N^2$. The unpolarized quark distribution functions $f_1^q(x)$ and $f_1^{\bar{q}}(x)$ are taken from the CTEQ5M global fits²⁴. The semi-inclusive $(e, e'h)$ cross section relates to the quark fragmentation function $D_q^h(z)$ and the total inclusive cross section σ_{tot} through:

$$\frac{1}{\sigma_{tot}} \frac{d\sigma(e, e'h)}{dz} = \frac{\sum_{q, \bar{q}} e_q^2 f_1^q(x) D_q^h(z)}{\sum_{q, \bar{q}} e_q^2 f_1^q(x)}. \quad (10)$$

For the light quark fragmentation functions $D^+(z)$ and $D^-(z)$, close to $Q^2 = 2.5$ GeV², we follow the parameterization of Kretzer, Leader and Christova²⁵:

$$\begin{aligned} D^+(z) &= 0.689z^{-1.039}(1-z)^{1.241} \\ D^-(z) &= 0.217z^{-1.805}(1-z)^{2.037} \end{aligned} \quad (11)$$

Existing data indicate that the fragmented products follow a Gaussian-like distribution in transverse momentum. For the $N(e, e'\pi)X$ reaction, recent HERMES preliminary data showed that the pion transverse momentum (P_\perp) distribution follows the form of $e^{(-aP_\perp^2)}$ with $a = 3.76$ (GeV/c)⁻², corresponding to an average quark transverse momentum of $\langle P_\perp^2 \rangle = 0.26$ (GeV/c)². We used this pion distribution and realistic spectrometer acceptances in a Monte Carlo simulation to estimate the count rates. The issue of pion decay is considered in the rate estimation, typical survival factor for a pion after a flight-path of 25.0 m in HMS is 0.82 for $p_\pi=2.2$ GeV/c. This rate estimate has been cross checked with an independent Monte Carlo rate estimate of Dr. D. Gaskell, the result agrees very well.

4.2 Beam time and coincidence rate

The beam time is chosen such that the statistical accuracies in the measured raw asymmetry in the $x = 0.34$ bin gives similar statistic accuracies for π^+ and π^- data. Table 2 lists the possible beam time request for the full proposal. Table 3 lists the coincidence rates in each x -bin.

Table 2: Beam time expectation.

P_{HMS} (GeV/c)	Time (Hour)
2.20 GeV, π^+ data collection	225
2.20 GeV, π^- data collection	600
Time on Pol. NH₃ Target	825 (34 days)
Target overhead and other overhead	255
Total Time	45 days

Table 3: Estimated coincidence rates for each x -bin, The average x values for each bin are listed.

$\langle x \rangle$	0.15	0.24	0.34	0.46
Rate π^+ (Hz)	0.72	0.58	0.41	0.22
Rate π^- (Hz)	0.49	0.35	0.23	0.11

5 Expected Results

5.1 Single-spin asymmetry

The expected statistical accuracies of proton single-spin asymmetry measurements are shown in Fig. 13. In $(e, e'\pi)$ reactions, the effects of radiative corrections are expected to be less serious than in the inclusive scattering. In addition, radiative corrections will not generate any single spin asymmetry at the leading order. Therefore, the effect of radiative corrections in this experiment is likely to be rather small.

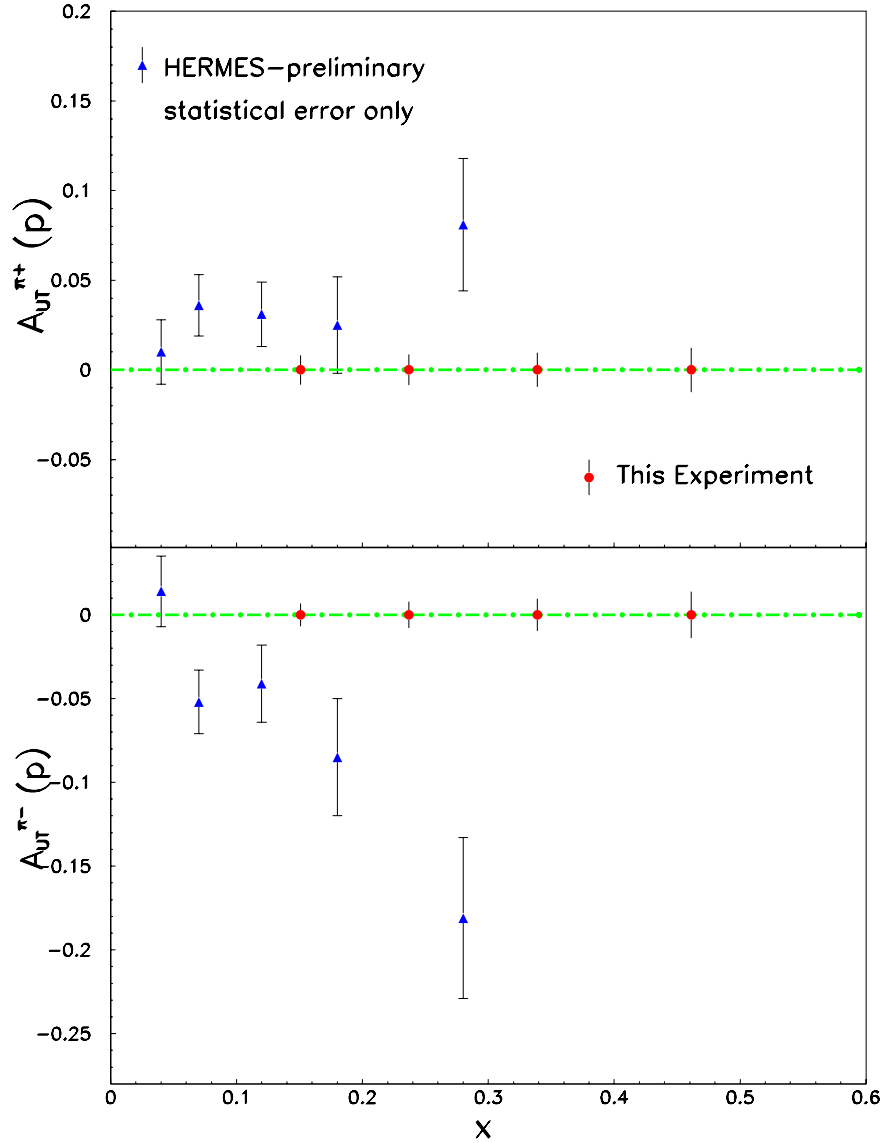


Figure 13: Expected statistical precision for $\vec{p}(e, e'\pi^+)X$ and $\vec{p}(e, e'\pi^-)X$ measurements, compared with the preliminary HERMES results (statistical error only).

The possible contamination of exclusive ρ production can be much eliminated by a combined cut on z and W' , according to our preliminary simulation study. The kinematics we chose in this experiment is very different from that of the HERMES. While this experiment focuses on the valence- x region and enforces $z \sim 0.5$, HERMES data sample is dominated by events from lower- x region and lower z region. A detailed Monte Carlo study will be included in the full proposal.

5.2 By-products

As by-products, charged kaon yields are expected to be about at the 10% level compared to the pion yields. Target single spin asymmetries of $\vec{p}(e, e'K^+)X$ and $\vec{p}(e, e'K^-)X$ reaction will also be extracted within the same data, since HMS will be instrumented to have good kaon particle ID. Coincidence data will also produce double-spin asymmetries A_{LT} on the $\vec{p}(e, e'\pi^+)X$ and $\vec{p}(e, e'\pi^-)X$ reaction, which is sensitive to the quark distribution of g_{1T} .

6 Summary

We propose to measure the target single spin asymmetry in the semi-inclusive deep-inelastic $\vec{p}(e, e'\pi^+)$ and $\vec{p}(e, e'\pi^-)$ reaction with a vertically polarized NH_3 target. A large array of calorimeter blocks, 50% extended from the existing BigCal, will be used as the electron detector, to provide out-of-plane angle coverage and to cover a large range of Collins angles $\phi_h + \phi_S$. The Sivers angle $\phi_h - \phi_S$, on the other hand will be optimized close to 90° . The variation of single spin asymmetry over this large range of Collins angle will provide a clear differentiation between the two competing mechanisms—the chiral-even Sivers effect and the chiral-odd Collins effect. This experiment will provide powerful constraints on the transversity distributions on both u -quark and d -quark in the valence region.

On the technical side, the design and development of a vertically polarized target, with a 5.1T super-conducting magnet to provide 80% target polarization, will be justified as a long term investment for the future Jefferson Lab physics program. The polarized target design and beamline development, although not an easy task, directly fit into the Jefferson Lab's 12 GeV upgrade. With the expected approval of the 12 GeV upgrade, a very rich transverse spin physics program is expected to take the center stage of JLab physics in the future.

We believe that this experiment will have strong impacts to the transversity physics. The success of this experiment will help to shape the future physics program at the upgraded JLab. The collaboration is eager to jump into the work of the target design, and additional funding support is crucial to the progress of the technical work. Working closely together with Oxford Instrumentation, we expected to finish a technical design report and cost estimation in six months. Once the design work has been finished, the manufacturing of the magnet will likely to take $18 \sim 24$ months.

We plan to submit a full proposal to PAC26, a total of 45 days of beam time in Hall C at 6 GeV will be requested in the full proposal.

References

1. See the recent review by V. Barone, A. Drago and P.G. Ratcliffe, *Phys. Rept.* **359** 1 (2002).
2. HERMES Collaboration, A. Airapetian *et al.*, *Phys. Rev. Lett.* **84**, 4047 (2000).
3. HERMES Collaboration, A. Airapetian *et al.*, *Phys. Rev. D* **64**, 097101 (2001).
4. V.A. Korotkov, W.-D. Nowak and K.A. Oganessian, *Eur. Phys. J. C* **18**, 639 (2001).
5. R.L. Jaffe, Proceedings of “Deep inelastic scattering off polarized targets, Physics with polarized protons at HERA”, Hamburg/Zeuthen 1997, p. 167-180, Report MIT-CTP-2685, hep-ph/9710465.
6. J.P. Ralston and D.E. Soper, *Nucl. Phys.* **B 152** (1979).
7. C. Bourrely, J. Soffer and O. V. Teryaev, *Phys. Lett.* **B420** (1998) 375, hep-ph/9710224.
8. J. Soffer, *Phys. Rev. Lett.* **74**, 1292 (1995).
9. J.C. Collins, *Nucl. Phys.* **B 396**, 161 (1993); *Nucl. Phys.* **B 420**, 565 (1994).
10. A.V. Efremov, O.G. Smirnova and L.G. Tkachev, *Nucl. Phys. Proc. Suppl.* **74**, 49 (1999).
11. A. Bravar for the SMC Collaboration, *Nucl. Phys. Proc. Suppl.* **79**, 520 (1999).
12. P. Mulders and R. D. Tangerman *Nucl. Phys.* **B 461**, 197 (1996)
13. A. Kotzinian, *Nucl. Phys.* **B 441**, 234 (1995).
14. D. Boer and P. Mulders, *Phys. Rev. D* **57**, 5780 (1998)
15. E. De Sanctis, W.-D. Nowak and K. A. Oganessian, *Phys. Lett.* **B 483**, 69 (2000).
16. K. A. Oganessian, H. R. Avakian, N. Bianchi and A. M. Kotzinian, hep-ph/9808368.
17. Stanley J. Brodsky, Dae Sung Hwang and Ivan Schmidt, *Phys. Lett.* **B 530**, 99 (2002).
18. J.C. Collins, *Phys. Lett.* **B 536**, 43 (2002).
19. D. Sivers, *Phys. Rev. D* **43**, 261 (1991).
20. X. Ji and F. Yuan, *Phys. Lett.* **B 543**, 66 (2002). A.V.Belitsky, *et al.*, hep-ph/0208038.
21. Bo-Qiang Ma, Ivan Schmidt and Jian-Jun Yang, *Phys. Rev. D* **65**, 034010 (2002), and hep-ph/0209114.
22. A. M. Kotzinian, *et al.*, hep-ph/9908466.
23. P. Degtiarenko, private communications, November 2003.
24. H. L. Lai, *et al.*, *Phys. Rev. D* **55**, 1280 (1997).
25. S. Kretzer, E. Leader and E. Christova, *Eur. Phys. J. C* **22**, 269 (2001).
26. HERMES Collaboration preliminary results (<http://www-hermes.desy.de>).